

Geophysical Research Letters®



RESEARCH LETTER

10.1029/2024GL114277

Key Points:

- We analyze volcanic vent distribution and calculate the Gravitational Potential Energy (GPE) in the Turkana Depression, East Africa
- GPE-related stresses resulting from variations in topography and (subordinately) crustal thickness control off-rift volcanism distribution
- Vent alignment within major volcanic fields responds to local, GPE-controlled stresses and not to the plate motion-driven stress field

Supporting Information:

Supporting Information may be found in the online version of this article.

Correspondence to:

G. Corti and D. Keir,
giacomo.corti@igg.cnr.it;
D.Keir@soton.ac.uk








Citation:

Corti, G., Muluneh, A., Stamps, D. S., Keir, D., Isola, I., Mazzarini, F., et al. (2025). Control of gravitational potential energy on the distribution of off-rift volcanic activity in the Turkana depression, East African rift. *Geophysical Research Letters*, 52, e2024GL114277. <https://doi.org/10.1029/2024GL114277>

Received 18 DEC 2024

Accepted 13 MAY 2025

Control of Gravitational Potential Energy on the Distribution of Off-Rift Volcanic Activity in the Turkana Depression, East African Rift

Giacomo Corti¹ , Ameha Muluneh^{2,3} , D. Sarah Stamps⁴ , Derek Keir^{5,6} , Ilaria Isola⁷, Francesco Mazzarini⁷ , Sascha Brune^{3,8} , and Daniele Maestrelli¹ 

¹Istituto di Geoscienze e Georisorse, Consiglio Nazionale delle Ricerche, Florence, Italy, ²MARUM Center for Marine Environmental Sciences, University of Bremen, Bremen, Germany, ³GFZ Helmholtz Centre for Geosciences, Potsdam, Germany, ⁴Department of Geosciences, Virginia Tech, Blacksburg, VA, USA, ⁵Dipartimento di Scienze della Terra, Università degli Studi di Firenze, Florence, Italy, ⁶School of Ocean and Earth Science, University of Southampton, Southampton, UK, ⁷Istituto Nazionale di Geofisica e Vulcanologia, Pisa, Italy, ⁸University of Potsdam, Potsdam, Germany

Abstract The distribution and alignment of volcanism in continental rifts is controlled by regional extensional stresses modulated by several factors such as structural inheritance, volcano edifice loading, and rift architecture. These interactions result in complex characteristics of rift-related volcanic features, which may be difficult to interpret considering the different controlling processes. The Turkana Depression (East Africa) exemplifies these complexities, showing an anomalous location of volcanic fields (outside the area of ongoing extension), with variable vent orientation. We analyze vent distribution in the Turkana Depression and calculate the stresses resulting from Gravitational Potential Energy (GPE). Our results show that West to East variations in topography and (subordinately) crustal thickness give rise to extensional GPE-related stresses East of Lake Turkana, where recent off-rift volcanism is localized. Within each different volcanic field, local GPE-related stresses control the arrangement of volcanic vents, which therefore do not respond to the regional (plate motion-driven) stress field.

Plain Language Summary Continents sometimes divide into two parts with a new ocean forming in between. This process happens along a rift valley (like in East Africa) where the tectonic plate stretches and thins, and where active volcanoes commonly form. However, the distribution of volcanoes near rift valleys is sometimes very complex and difficult to interpret, since it is controlled by many different parameters. They most commonly form along faults and fractures in the rift, but forces created by the weight of the uplifted rift valleys sides and high volcanoes, as well as pressure from subsurface magma chambers, can also influence their formation. In this paper, we study the Turkana depression in East Africa to understand the control on volcanic activity by the forces created by the difference in topography and crustal thickness between the uplifted rift sides and the downthrown Turkana depression. Our calculations show that forces caused by changes in topography are the main control on the movement of magma to the surface, and therefore control where volcanic fields form, and the shape that they form in. These results are important since a similar process may control volcanics activity in others rift valleys around the world.

1. Introduction

Understanding the distribution and alignment of volcanic activity and its governing factors are critical in the analysis of continental rifting and break-up. Different studies have shown that magma migration, emplacement and final eruption may not always respond to the imposed regional tectonic (plate motion-driven) stress field, but instead be controlled by local processes such as structural inheritance, rift architecture, loading by volcanic edifices, and unloading by extension and pressure generated by a magma reservoir (e.g., Maccaferri et al., 2014; C. K. Morley, 2020; Wadge et al., 2016). The diverse controls on the stress field result in complex spatial distributions of fissures and vents, which may deviate from the regional extension-orthogonal orientation and potentially change during rift evolution. Therefore, explaining the distribution of volcanic activity during rifting and its relation with regional/local stress fields and their controlling factors is challenging.

The Turkana Depression in East Africa (Figure 1) exemplifies these complexities, showing an anomalous distribution of volcanism with several important volcanic centers located outside the area of ongoing extension, and

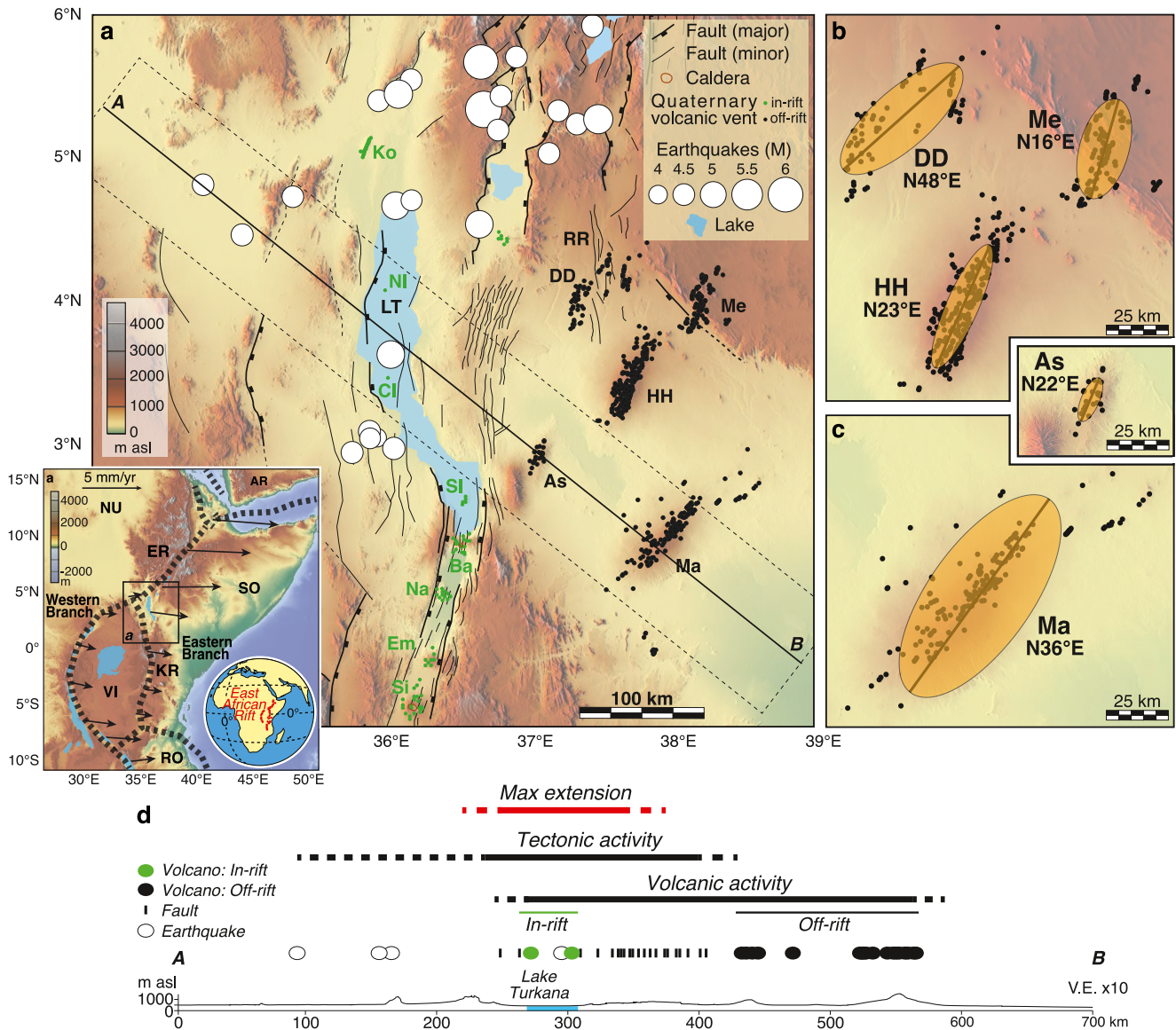


Figure 1. (a) Faults, seismicity, and Pleistocene-Holocene volcanic vents in the Turkana Depression superimposed on a SRTM (Nasa Shuttle Radar Topography Mission) digital elevation model. Seismicity is from U.S. Geological Survey National Earthquake Information Center catalog (1900 to present; citation needed for the NEIC catalog, <https://earthquake.usgs.gov/earthquakes/search/>). Green dots illustrate in-axis volcanoes (Em: Emuruangogolak, Ba: Barrier, CI: Central Island, Ko: Korath range, Na: Namarunu, Si: Silali, SI: South Island); black dots illustrate off-rift volcanic fields (As: Asie; DD: Dilo-Dukana; HH: Hurri Hills; Ma: Marsabit; Me: Mega). LT: Lake Turkana; RR: Ririba Rift. Inset in the bottom left corner illustrate the present-day plate kinematics of the East African Rift. Black arrows show relative motions with respect to a stable Nubian reference frame according to the best fit model of Saria et al. (2014). Black dashed lines indicate plate and microplate boundaries from Stamps et al. (2021). AR: Arabian plate; ER: Ethiopian Rift; KR: Kenyan Rift; NU: Nubian plate; SO: Somalian plate; RO: Rovuma microplate; VI: Victoria microplate. (b, c) Details of vent distribution in the different volcanic fields, illustrated as ellipses that are derived by applying Principal Component Analysis (PCA; Mazzarini et al., 2016) to the original data sets (vent location in UTM coordinates -WGS84 datum, available as open access database (Isola et al., 2024)). PCA describes the ellipse containing 95% of the data set and gives the azimuth of each ellipse's major axis. Numbers below the labels of the volcanic field name indicate the orientation of the ellipse's maximum axis. (d) Distribution of tectonic and volcanic activity across the Turkana Depression (location of cross-section in panel a). The red line ("Max extension") indicates the area of maximum active extension and the modern-day plate boundary constrained from the synthesis of seismic and geodetic results by Musila et al. (2023). VE: vertical exaggeration.

showing variable orientation of vents in the different volcanic fields (e.g., Mazzarini & Isola, 2022). Specifically, it is unclear why off-rift volcanism occurs only East of the rift axis. Also, the field alignments are enigmatic as they are neither parallel to the rift trend nor perpendicular to the local extension direction. Lithospheric characteristics (e.g., rheology, thickness, strength) and their lateral variations, magma dynamics (genesis and migration processes), crustal properties (e.g., presence of inherited structures), and local/regional stress fields

Table 1
Characteristics of Off-Rift Volcanic Fields in the Turkana Depression

Name	Type of activity	Dominant composition	Age of latest activity (Ma)
Dilo–Dukana (DD)	Cinder and scoria cones, maars	Basanites	0.135
Mega (Me)	Cinder and scoria cones, maars	Basanites	Holocene
Hurri Hills (HH)	Cinder and scoria cones, maars	Basalts, Basanites	0.5
Asie (As)	Cinder cones, maars	Basalts, Basanites	0.4
Marsabit (Ma)	Cinder cones, maars	Basalts, Basanites	<1

have been suggested to influence the spatial distribution and variability in orientation of volcanic features in the region (e.g., Franceschini et al., 2020; Mazzarini & Isola, 2022). However, the primary controls on the distribution and alignment of volcanic activity in the Turkana depression still remains unclear.

In this paper, we provide additional constraints on these complex processes by focusing on the volcanic activity located outside the rift valley and provide a comprehensive analysis of its distribution and orientation. We compute the Gravitational Potential Energy (GPE) related to variations in crustal thickness and topography in the Turkana depression and show that this parameter has a strong control on magma migration and emplacement by controlling the location and alignment of volcanic vents in the area.

2. Tectonic Setting

The Turkana depression is a low-land located between the uplifted East African and Ethiopian domes, and is the region of interaction between the Main Ethiopian Rift (MER) and Kenyan Rift (Figure 1). These two rifts are part of the Eastern Branch of the East African Rift (EAR), a system of 80–100 km-wide rift valleys extending for several thousand kilometers in the Eastern part of the African continent (Figure 1). The EAR marks the incipient boundary between the Nubian and Somalian plates, that are diverging at rates of 3–5 mm/year in a roughly E-W direction (Saria et al., 2014).

The current morphology of the Turkana depression does not correspond to a narrow rift valley dominated by large fault escarpments. Instead, the area is characterized by low relief marked by numerous, small-offset normal faults and volcanic centers widespread over a wide region (Figure 1). Seismicity and geodetic analysis indicate that only a localized part of the rift (i.e., Lake Turkana basin) is currently active (Knappe et al., 2020; Musila et al., 2023; Sullivan et al., 2024), although Pleistocene-Holocene volcanoes are distributed over a more than 300 km-wide portion of the depression (Figure 1; e.g., Mazzarini & Isola, 2022). The atypical width of the Turkana depression and its anomalous low topography are believed to be a consequence of the interplay between the propagation and interaction of the two main rift systems in the area (MER, Kenyan Rift) and the transversal (roughly NW-SE-trending) pre-existing Mesozoic basin of the Anza graben (e.g., Benoit et al., 2006; Brune et al., 2017; Corti et al., 2019; Ebinger et al., 2000; C. Morley & Boone, 2025; Sullivan et al., 2024).

Rifting in the Turkana depression has been accompanied by significant volcanism (Figure 1; Figure S1 in Supporting Information S1). The youngest major pulse was in the Pliocene and mostly basaltic, which initially occurred as widespread fissural flows and then followed by building of large shield volcanoes (e.g., Asie, Hurri Hills, Marsabit; Figure S1 in Supporting Information S1; Rooney, 2020). This basaltic pulse was in turn followed by more localized Pleistocene-Holocene activity. In particular, this recent volcanism characterized the actively deforming axial portions of the northern Kenya Rift and the Lake Turkana basin where several volcanic centers with Holocene activity (e.g., North Island, Central Island, South Island, Barrier) are present (in-axis volcanoes, Figure 1; Figure S1 in Supporting Information S1). These volcanic centers are characterized by products showing a wide range of magma compositions including dominant basalts and trachytes with subordinate silicic pyroclastics and rhyolites (Rooney et al., 2022, and references therein). Significant recent volcanic activity has also occurred outside the actively deforming zone, with different volcanic fields exhibiting aligned monogenetic cones/maars and associated flows, well-developed on top of the Pliocene shield volcanoes (e.g., Hurri Hills, Marsabit) or between them (e.g., Dilo-Dukana, Mega; off-rift volcanoes, Figure 1; Figure S1 in Supporting Information S1; Table 1). These centers characterize the region East of Lake Turkana, with no recent volcanism West of this basin, therefore marking an asymmetric distribution of recent volcanic activity with respect to the

locus of active deformation in the Turkana depression (Figure 1). The off-rift volcanism is characterized by predominant basaltic and basanitic composition with activity dominated by cinder and scoria cones and maars (Table 1; Mazzarini & Isola, 2022 and references therein). Being away from the region of focused active extension, this activity is unrelated to the main rift structures, as exemplified in the Ririba rift (Figure 1), where the abandonment of extension-related faults at the Pliocene-Pleistocene boundary has been followed by emplacement of the Dilo-Dukana vents which cut the inactive normal faults (e.g., Corti et al., 2019; Franceschini et al., 2020). Both lithosphere and asthenosphere control has been suggested to influence the overall locus of volcanism. Mazzarini and Isola (2022) suggest pre-existing structures in the extended crust and rheological heterogeneities in the mantle lithosphere exert primary influence on the distribution of recent volcanic activity in the Turkana Depression. In contrast, Kounoudis et al. (2021) propose that melt supply is focused in the uppermost asthenosphere and lower lithosphere in zones where the plate has been thinned by past and ongoing rifting.

Crustal thickness of the Turkana Depression has been constrained using receiver functions (Ogden et al., 2023). The results show the crust is ~40 km thick beneath the rift flanks, and thins to 20–30 km beneath most of the rift (Ogden et al., 2023). Specifically, the crust is thinnest (<25 km thick beneath the actively deforming Lake Turkana basin. V_p/V_s is ~1.74 throughout the depression and beneath the rift flanks indicative of normal continental crust, suggesting that the volume of magma intrusion is relatively low. Instead plate stretching and faulting accounts for most of the extension over the rift history (Ogden et al., 2023). The limited volumes of Cenozoic magmatism are also consistent with seismic tomography which broadly shows lithosphere seismic velocities that are relatively normal, consistent with limited evidence for thermal modification (Kounoudis et al., 2021). The seismic tomography only shows evidence for partial melt in the lithosphere and upper asthenosphere in limited areas beneath the rift and Eastern rift flank, which correlate spatially to the Pleistocene-Holocene volcanism both in- and off-rift (Kounoudis et al., 2021). Localized zones of magma intrusion and deformation document a recent transition from boundary faulting to magma-driven axial extension in the actively deforming Lake Turkana basin (Muirhead et al., 2022).

3. Methods

3.1. Analysis of Vent Alignment

Our vent mapping relied on 3 sources: (a) analyzing SRTM digital elevation models with a cell size of 30 m (<http://www2.jpl.nasa.gov/srtm/>), (b) interpreting panchromatic satellite images with pixel resolution of 2.5–20 m by using Google Earth (<http://earth.google.com/>), and (c) integrating previous work by Mazzarini and Isola (2022). The location of monogenetic vents (cones) with a preserved recognizable volcanic morphology is illustrated in Figure 1, for both in-axis and off-rift volcanic fields, and available as open access database (Isola et al., 2024). Vents with a diameter smaller than a few pixels (i.e., <60 m), disrupted vents (vents without a well-preserved morphology), and vents covered by younger volcanic products have been filtered out.

The shape of a volcanic field has been assessed by analyzing the vent locations (UTM coordinates) through Principal Component Analysis (PCA), which is a linear method for dimensionality reduction (see Mazzarini et al., 2016 and references therein). The PCA provides ellipses containing 95% of the data set and gives the azimuth of each ellipse's major axis, which corresponds to the main alignment of the volcanic field. The results of this PCA analysis has been successively compared with analysis in the Geographic Information System software QGIS for further validation.

Specifically, the Standard Deviational Ellipse tool is used in QGIS to investigate point patterns, which shows a summary of the distribution as a standard deviation ellipse constructed following the Yuill (1971) method. The tool provides the DSE polygon and the attributes that characterize the ellipse: $mean_x$, $mean_y$, $major_{sd}$ (Standard Deviation along the major axis), $minor_{sd}$ (Standard Deviation along the minor axis that is normal to the major axis), $major_{angle}$ (rad) (major axis angle in radians counter-clockwise relative to x/East), $direction_{deg}$ ("compass" direction - degrees clockwise relative to north), and eccentricity ($\sqrt{1 - b^2/a^2}$). These results are compared with the PCA analysis for cross validation.

3.2. Gravitational Potential Energy (GPE)

Calculation of the vertically averaged stress available to break an initially thick and cold lithosphere suggests that gravitational forces are not sufficient to induce rifting and that an additional weakening mechanism is required,

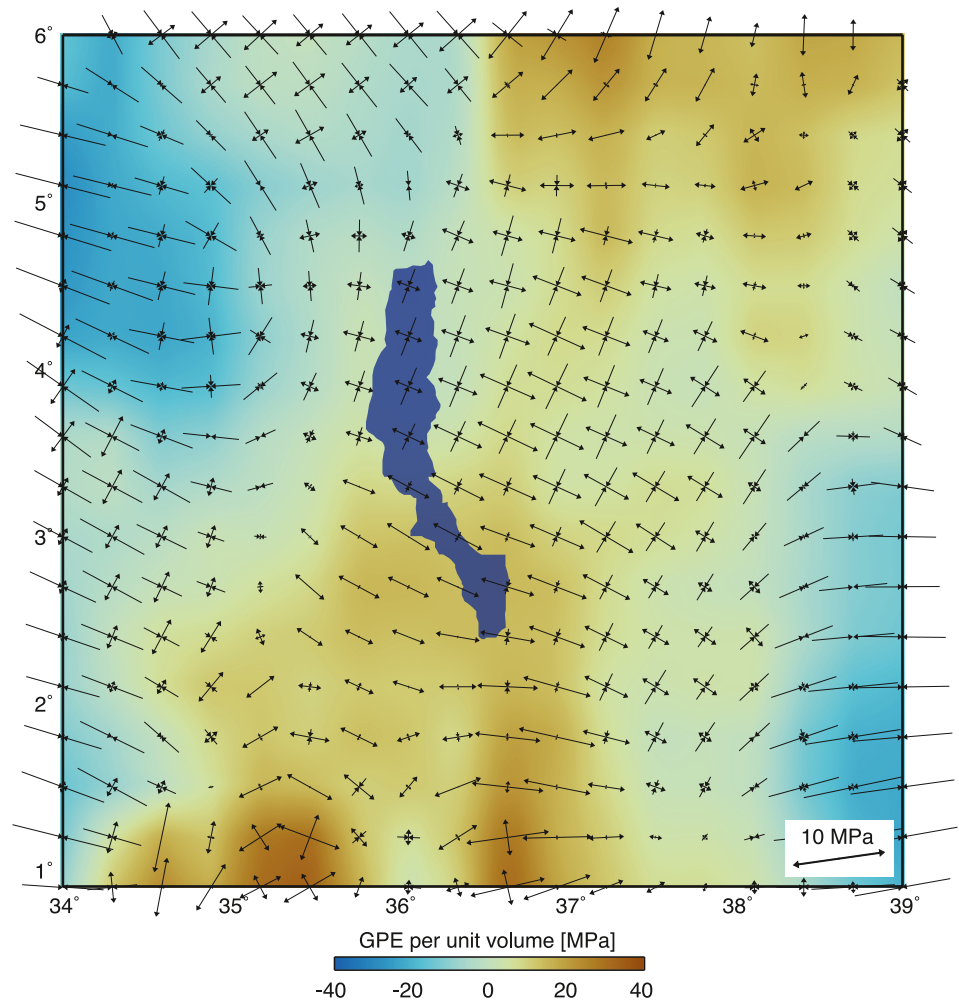


Figure 2. Gravitational potential energy (GPE) per unit volume in the Turkana Depression for a layer thickness of 100 km. See text for details. The arrows show the principal (compression and extension) axes of the deviatoric stress. Negative and positive values indicate compression and extension, respectively.

primarily from the effects of melt (W. R. Buck, 2004, 2006). However, once the rift has localized, the stress from variations in gravitational potential energy (GPE), which is on the order of few tens of megapascals, can drive extension (Stamps et al., 2010, 2014). Here we use a method proposed by Flesch et al. (2007) and implemented in Hirschberg et al. (2019) to calculate vertically averaged deviatoric stress arising from gradients of GPE. We calculate the GPE gradient per unit volume over a depth of z using the following equation:

$$\text{GPE} = 1/L \int_{-h}^L \int_{-h}^z g\rho(z') dz' dz \quad (1)$$

where g is acceleration due to gravity, ρ is the rock density at depth z' , h is the elevation, and L is the thickness of the lithosphere over which the GPE is averaged, which is ~ 100 km (Ghosh et al., 2019; Illsley-Kemp et al., 2017; Stamps et al., 2010). Equation 1 is integrated from Earth's surface ($z = -h$) to the base of the column ($z = L$) (Hirschberg et al., 2019). The calculated GPE considers the contribution of the crust and mantle down to 100 km (Figure 2), which comprises the entire lithosphere in our study area (Afonso et al., 2022). Figure 2 illustrates the gravitational potential energy per unit volume calculated for a compensation depth of 100 km and principal axes (compression and extension) of the deviatoric stress due to gravity (Hirschberg et al., 2019).

For the Turkana area, we use crustal and mantle densities of 2,700 and 3,200 kg/m³, respectively. Previous studies (e.g., Stamps et al., 2014) demonstrated that both uncompensated cases, where the density of the mantle is uniform, and compensated cases, where calculations are made with laterally varying density, exhibit similar magnitudes of GPE gradients in the EARS. The GPE gradient was calculated in a 0.3° rectangular grid (Figure 2). The accuracy of GPE gradients is dependent on the accuracy of the crustal thickness estimates. We initially use a recent crustal thickness estimate constrained by receiver functions (Figure S2 in Supporting Information S1; Ogden et al., 2023). Ogden et al. (2023) show that the crust in the Turkana area is thinner (<25 km) in the vicinity of and around Lake Turkana and gets thicker in the surrounding region. The thinner crust coincides with the region of highest strain rate observed using geodesy (Knappe et al., 2020). We also employ the CRUST1.0 model (Laske et al., 2013) and perform an alternative calculation to assess the uncertainty of the GPE gradients (see Figures S3 and S4 in Supporting Information S1). To evaluate the impact of the selected compensation depth (100 km), we conduct additional calculations with compensation depths of 75 and 125 km (Figure S5 in Supporting Information S1). We also include calculations with a fixed Moho depth of 30 Km (and variable topography), and a fixed topography (and variable crustal thickness), in order to isolate the effect of topography and crustal thickness on the GPE pattern (Figure S6 in Supporting Information S1).

4. Results and Discussion

Analysis of vents in the different off-rift fields indicate that the main axis of the distribution ellipses displays variable orientation (Figures 1 and 3a): from N48°E for Dilo-Dukana to N16°E for Mega. The value of the Dilo-Dukana field may be influenced by the superposition of three different sub-fields in this area (see Corti et al., 2019; Figure S7 in Supporting Information S1). Conversely, all of the in-rift volcanic vents show a constant alignment with the rift trend (N10°E to N20°E; Figure 1; Figure S8 in Supporting Information S1), with Namarunu (which is oriented roughly NW-SE) being the only exception.

Similarly, the GPE-related stresses display important spatial variations within the Turkana depression: in general, stresses are mostly compressional West of Lake Turkana and extensional in a wide region East of it (Figures 2, 3a, and 3b). The GPE-controlled least compressive stress is mostly oriented ESE-WNW East of Lake Turkana but rotates to roughly E-W or NW-SE in places. The comparison between the maximum horizontal compressive stress (SHmax) obtained using CRUST1.0 and Ogden et al. (2023) crustal thickness models (see Figure S4 in Supporting Information S1) shows that both crustal models indicate similar magnitudes and directions of GPE gradients in the Turkana area with the exceptions of the Northwestern and Eastern parts of the study area that are situated away from the volcanic centers discussed in this paper. The magnitude of deviatoric stress associated with the GPE gradients (the length of the arrows in Figure 2) ranges from 0 to 15 MPa, which is a similar range in the magnitudes of GPE related stress from previous studies in East Africa (Mahatsente & Coblenz, 2015; Stamps et al., 2010). Our maximum values are located in the high topography areas NE and SW of the Turkana depression; the minimum values occur within the depression, NW and SE of Lake Turkana. Alternative calculations indicate that GPE gradients exhibit minimal variation for different compensation depths (Figure S5 in Supporting Information S1). In the area of interest, the orientation of the GPE gradients shown in Figure 2 agrees well with a variable topography for a fixed crustal thickness of 30 km (Figure S6 in Supporting Information S1), indicating that topography plays a dominant role on their distribution.

Comparison between the style of GPE-related stresses and the distribution of off-rift volcanic vents displays a very good match (Figure 3c; Figure S8 in Supporting Information S1). Primarily, all the off-rift volcanism in the Turkana depression is located East of Lake Turkana where GPE gradients create tensional stresses that favor magma ascent and eruption; no volcanism is observed West of Lake Turkana in agreement with the compressional state of stress induced by GPE gradients (Figure 3b). East of Turkana, the off-rift volcanism does also correlate to focused supply of melt to regions of thinned lithosphere from prior Mesozoic rifting (Kounoudis et al., 2021). However, regions of thinned lithosphere West of Turkana show no evidence for significant mantle melting. Enhanced melt migration in regions of high GPE gradients would create pressure gradients in the lower plate and asthenosphere which localize melt flow and melt extraction (Sleep, 1997), explaining the asymmetry to the East of both off-rift melt supply and volcanism.

In all of the different volcanic fields, the long axis of the ellipses of vent distribution are sub-orthogonal to the GPE-induced least compressive stress. This orthogonal match with least compressive stress directions is also observed in the Dilo-Dukana field by considering the superposition of the three different sub-fields (Figures S7

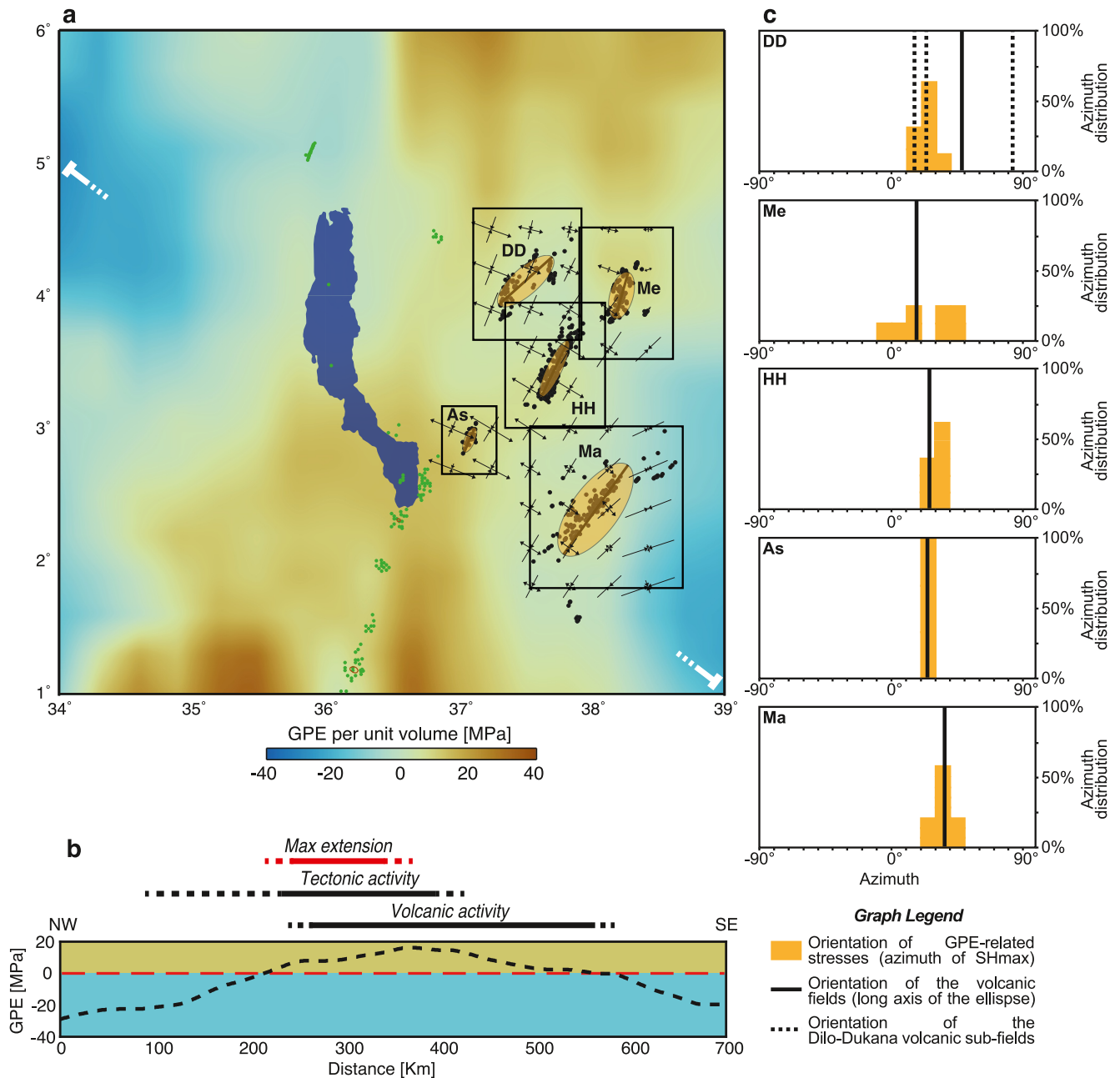


Figure 3. (a) Relationship between gravitational potential energy (GPE) and the distribution of volcanic vents in the Turkana Depression. (b) Distribution of GPE across the Turkana Depression (cross-section A-B in Figure 1 and panel a), along with distribution of tectonic and volcanic activity as in Figure 1. (c) Graphs showing the distribution of the orientation of GPE-related stresses expressed as the azimuth of SHmax (i.e., orthogonal to SHmin) within the volcanic fields and surroundings (arrows in left panel), black lines indicate the orientation of the volcanic fields (expressed as the direction of the long axis of the field ellipse), and dashed lines indicate the orientation of the sub-fields in the Dilo area (0° is North, 90° in East and -90° is West).

and S8 in Supporting Information S1). No relations are observed between off-rift vent distribution and the plate-scale direction of extension (from GNSS data; Knappe et al., 2020; Musila et al., 2023), whereas a closer match is observed with local stress directions from borehole breakout data (Figure S8 in Supporting Information S1).

In-rift vent alignments are consistently oriented NNE-SSW; only the roughly NW-SE-oriented Namarunu volcanic field is oblique to regional extension. In contrast to what is observed for the off-rift volcanic fields, there is no clear relation between in-rift vent alignments and the GPE-induced least compressive stress (Figure S8 in Supporting Information S1). Where available, plate scale velocity vectors from GNSS data and T-axes of

available focal mechanisms show a closer match with in-rift vent orientation (Figure S8 in Supporting Information S1).

This comparison indicates that the off-rift volcanic vent alignments respond to local GPE-induced stresses, which are in turn primarily controlled by variations in topography. Conversely, in-rift volcanic fields respond directly to regional plate motion-driven stresses (Muirhead et al., 2022). In the case of Namarunu, the deviation may be related to the control exerted by pre-existing structures. Control by GPE-related stresses have been suggested for the post-rift (Late Pleistocene-Holocene) volcanism at the southernmost tip of the MER (Franceschini et al., 2020). In this area, the Ririba rift has become inactive during the Pliocene when deformation jumped westwards into the Lake Turkana basin (Corti et al., 2019). After rift abandonment, plate motion-related extensional stresses faded and became subordinate to GPE-related stresses, which therefore controlled the emplacement of the recent volcanism in the area (Franceschini et al., 2020). Our current analysis allows us to extrapolate this control of GPE-induced stresses on vent alignment to all of the off-rift volcanism of the Turkana depression, East of the area where deformation is currently localized and where tectonic stresses are subordinate. Within each of the off-rift volcanic fields, magma ascent may have created new fractures or exploited inherited lithospheric structures or strong rheological contrasts (Mazzarini & Isola, 2022) optimally oriented to the local, GPE-related stress field. Overall, this indicates that care should be used when using off-rift volcanism -in terms of vent alignment and/or elongation of the volcanic fields-for the definition of the far-field (i.e., plate-scale) stress field.

5. Conclusions

We have analyzed the complex distribution of volcanism in the Turkana Depression, East Africa, where several prominent volcanic fields are located outside the area of focused, ongoing extension and show variable orientations of eruptive vents. We show that variations in topography and (subordinately) crustal thickness give rise to extensional stresses resulting from Gravitational Potential Energy (GPE) East of Lake Turkana; these extensional stresses allow magma to ascend to the surface, causing recent off-rift volcanism to be localized in this area. The orientation of vents in the major volcanic fields (e.g., Hurri Hills, Marsabit) is controlled by the GPE-related stress field. Specifically, alignments of eruptive vents are consistently perpendicular to the local, GPE-controlled least compressive stress. These findings indicate that stresses imposed by topography and the resulting GPE may be a primary factor in controlling the distribution of volcanism and the arrangement of volcanic vents and fissures, which may therefore not respond to the imposed regional (plate motion-driven) stress field.

Data Availability Statement

The data set of volcanic vents used in this research is freely available in the in-text citation (Isola et al., 2024), under Creative Commons Attribution 4.0 International License. The crustal thickness models used to compute the GPE gradient in Turkana can be found in Ogden et al. (2023) and CRUST1.0: <https://igppweb.ucsd.edu/~gabi/crust1.html>. We use the matlab code written by Hirschberg and colleagues (Hirschberg et al., 2019), which can be downloaded here: <https://github.com/hamishhirschberg/stress-modelling>.

Acknowledgments

We thank two anonymous Reviewers for the constructive comments that helped to improve this work. This research was partly supported by the European Union's H2020 LEAP-RE project. We also kindly acknowledge the support of the European Plate Observing System (EPOS) and the Joint Research Unit (JRU) EPOS Italia. A. M. has been funded by the German Research Foundation DFG (project no. 537025018). D.K. is partially supported through NERC Grant NE/L013932/1. S.B. has been funded by the European Union (ERC, EMERGE, 101087245).

References

- Afonso, J. C., Ben-Mansour, W., O'Reilly, S. Y., Griffin, W. L., Salajegheh, F., Foley, S., et al. (2022). Thermochemical structure and evolution of cratonic lithosphere in central and southern Africa. *Nature Geoscience*, 15(5), 405–410. <https://doi.org/10.1038/s41561-022-00929-y>
- Benoit, M. H., Nyblade, A. A., & Pasyanos, M. E. (2006). Crustal thinning between the Ethiopian and East African plateaus from modeling Rayleigh wave dispersion. *Geophysical Research Letters*, 33(13), L13301. <https://doi.org/10.1029/2006GL025687>
- Brune, S., Corti, G., & Ranalli, G. (2017). Controls of inherited lithospheric heterogeneity on rift linkage: Numerical and analogue models of interaction between the Kenyan and Ethiopian rifts across the Turkana depression. *Tectonics*, 36(9), 1767–1786. <https://doi.org/10.1002/2017TC004739>
- Buck, W. R. (2004). Consequences of asthenospheric variability on continental rifting. In G. D. Karner, B. Taylor, N. W. Droscholl, & D. L. Kohlstedt (Eds.), *Rheology and Deformation of the Lithosphere at Continental Margins* (pp. 1–30). Columbia University Press. <https://doi.org/10.7312/karn12738-002>
- Buck, W. R. (2006). The role of magma in the development of the Afro-Arabian rift system. In G. Yirgu, C. J. Ebinger, & P. K. H. Maguire (Eds.), *The Afar Volcanic Province within the East African Rift System: Geological* (Vol. 259, pp. 43–54). Society of London Special Publication. <https://doi.org/10.1144/gsl.sp.2006.259.01.05>
- Corti, G., Cioni, R., Franceschini, Z., Sani, F., Scaillet, S., Molin, P., et al. (2019). Aborted propagation of the Ethiopian rift caused by linkage with the Kenyan rift. *Nature Communications*, 10(1), 1309. <https://doi.org/10.1038/s41467-019-09335-2>
- Ebinger, C. J., Yemane, T., Harding, D., Tesfaye, S., Kelley, S., & Rex, D. C. (2000). Rift deflection, migration, and propagation: Linkage of the Ethiopian and Eastern rifts, Africa. *Geological Society of America Bulletin*, 112(2), 163–176. [https://doi.org/10.1130/0016-7606\(2000\)112<0163:rdmapl>2.3.co;2](https://doi.org/10.1130/0016-7606(2000)112<0163:rdmapl>2.3.co;2)

- Flesch, L. M., Holt, W. E., Haines, A. J., Wen, L., & Shen-Tu, B. (2007). The dynamics of Western North America: Stress magnitudes and the relative role of gravitational potential energy, plate interaction at the boundary and basal tractions. *Geophysical Journal International*, 169(3), 866–896. <https://doi.org/10.1111/j.1365-246x.2007.03274.x>
- Franceschini, Z., Cioni, R., Scaillet, S., Corti, G., Sani, F., Isola, I., et al. (2020). Recent volcano-tectonic activity of the Ririba rift and the evolution of rifting in South Ethiopia. *Journal of Volcanology and Geothermal Research*, 402, 106989. <https://doi.org/10.1016/j.jvolgeores.2020.106989>
- Ghosh, A., Holt, W., & Bahadori, A. (2019). Role of large-scale tectonic forces in intraplate earthquakes of central and eastern North America. *Geochemistry, Geophysics, Geosystems*, 20(4), 2134–2156. <https://doi.org/10.1029/2018GC008060>
- Hirschberg, H., Lamb, S., & Savage, M. K. (2019). Strength of an obliquely convergent plate boundary: Lithospheric stress magnitudes and viscosity in New Zealand. *Geophysical Journal International*, 216(2), 1005–1024. <https://doi.org/10.1093/gji/ggy477>
- Illsley-Kemp, F., Savage, M. K., Keir, D., Hirschberg, H., Bull, J. M., Gernon, T. M., et al. (2017). Extension and stress during continental breakup: Seismic anisotropy of the crust in Northern Afar. *Earth and Planetary Science Letters*, 477, 41–51. <https://doi.org/10.1016/j.epsl.2017.08.014>
- Isola, I., Mazzarini, F., Corti, G., & Maestrelli, D. (2024). Database of Quaternary volcanic vents in the Turkana depression [Dataset]. *Zenodo*. <https://doi.org/10.5281/zenodo.14505741>
- Knappe, E., Bendick, R., Ebinger, C. J., Birhanu, Y., Lewi, E., Floyd, M., et al. (2020). Accommodation of East African rifting across the Turkana depression. *Journal of Geophysical Research*, 125(2), e2019JB018469. <https://doi.org/10.1029/2019JB018469>
- Kounoudis, R., Bastow, I. D., Ebinger, C. J., Ogden, C. S., Bendick, R., Ayele, A., et al. (2021). Body wave tomographic imaging of the Turkana depression: Implications for rift development and plume-lithosphere interactions. *Geochemistry, Geophysics, Geosystems*, 22(8), e2021GC009782. <https://doi.org/10.1029/2021GC009782>
- Laske, G., Masters, G., Ma, Z., & Pasyanos, M. (2013). Update1.0—A 1-degree global model of Earth's crust. In *EGU General Assembly Conference Abstracts* (Vol. 15, p. EGU2013-2658).
- Maccaferri, F., Rivalta, E., Keir, D., & Acocella, V. (2014). Off-rift volcanism in rift zones determined by crustal unloading. *Nature Geoscience*, 7(4), 297–300. <https://doi.org/10.1038/ngeo2110>
- Mahatsente, R., & Coblenz, D. (2015). Ridge-push force and the state of stress in the Nubia-Somalia Plate system. *Lithosphere*, 7(5), 503–510. <https://doi.org/10.1130/L441.1>
- Mazzarini, F., & Isola, I. (2022). Quaternary off-rift volcanism along a section of the East African Rift System (EARS), from the South Ethiopia to the south Kenya. *Italian Journal of Geosciences*, 141(3), 334–347. <https://doi.org/10.3301/ijg.2022.19>
- Mazzarini, F., Le Corvec, N., Isola, I., & Favalli, M. (2016). Volcanic field elongation, vent distribution, and tectonic evolution of a continental rift: The main Ethiopian rift example. *Geosphere*, 12(3), 706–720. <https://doi.org/10.1130/GES01193.1>
- Morley, C. K. (2020). Early syn-rift igneous dike patterns, northern Kenya Rift (Turkana, Kenya): Implications for local and regional stresses, tectonics, and magma-structure interactions. *Geosphere*, 16(3), 890–918. <https://doi.org/10.1130/ges02107.1>
- Morley, C. K., & Boone, S. C. (2025). Inception and evolution of the Turkana depression: A review from the perspective of the longest-lived sector of the East African rift. *Journal of African Earth Sciences*, 227, 105625. <https://doi.org/10.1016/j.jafrearsci.2025.105625>
- Muirhead, J. D., Scholz, C. A., & Rooney, O. T. (2022). Transition to magma-driven rifting in the South Turkana basin, Kenya: Part 1. *Journal of the Geological Society*, 179(6). <https://doi.org/10.1144/jgs2021-159>
- Musila, M., Ebinger, C. J., Bastow, I. D., Sullivan, G., Oliva, S. J., Knappe, E., et al. (2023). Active deformation constraints on the Nubia-Somalia Plate boundary through heterogeneous lithosphere of the Turkana depression. *Geochemistry, Geophysics, Geosystems*, 24(9), e2023GC010982. <https://doi.org/10.1029/2023GC010982>
- Ogden, C. S., Bastow, I. D., Ebinger, C., Ayele, A., Kounoudis, R., Musila, M., et al. (2023). The development of multiple phases of superposed rifting in the Turkana depression, East Africa: Evidence from receiver functions. *Earth and Planetary Science Letters*, 609, 118088. <https://doi.org/10.1016/j.epsl.2023.118088>
- Rooney, T. O. (2020). The Cenozoic magmatism of East Africa: Part II—Rifting of the mobile belt. *Lithos*, 360–361, 105291. <https://doi.org/10.1016/j.lithos.2019.105291>
- Rooney, T. O., Wallace, P. J., Muirhead, J. D., Chiasera, B., Steiner, R. A., Girard, G., & Karson, J. A. (2022). Transition to magma-driven rifting in the South Turkana basin: Part 2. *Journal of the Geological Society*, 2021–160. <https://doi.org/10.1144/jgs2021-160>
- Saria, E., Calais, E., Stamps, D. S., Delvaux, D., & Hartnady, C. J. H. (2014). Present-day kinematics of the East African rift. *Journal of Geophysical Research: Solid Earth*, 119(4), 3584–3600. <https://doi.org/10.1002/2013jb010901>
- Sleep, N. H. (1997). Lateral flow and ponding of starting plume material. *Journal of Geophysical Research*, 102(B5), 10001–10012. <https://doi.org/10.1029/97jb00551>
- Stamps, D. S., Flesch, L. M., & Calais, E. (2010). Lithospheric buoyancy forces in Africa from a thin sheet approach. *International Journal of Earth Sciences*, 99(7), 1525–1533. <https://doi.org/10.1007/s00531-010-0533-2>
- Stamps, D. S., Kreemer, C., Fernandes, R., Rajaonarison, T. A., & Rambolamanana, G. (2021). Redefining East African rift system kinematics. *Geology*, 49(2), 150–155. <https://doi.org/10.1130/G47985.1>
- Stamps, S., Flesch, L., Calais, E., & Ghosh, A. (2014). Current kinematics and dynamics of Africa and the East African rift system. *Journal of Geophysical Research: Solid Earth*, 119(6), 5161–5186. <https://doi.org/10.1002/2013JB010717>
- Sullivan, G., Ebinger, C. J., Musila, M., Perry, M., Kraus, E. R., Bastow, I., & Bendick, B. (2024). Kinematics of rift linkage between the eastern and Ethiopian rifts in the Turkana depression, Africa. *Basin Research*, 36(5), e12900. <https://doi.org/10.1111/bre.12900>
- Wadge, G., Biggs, J., Lloyd, R., & Kendall, J. M. (2016). Historical volcanism and the state of stress in the East African rift system. *Frontiers in Earth Science*, 4, 86. <https://doi.org/10.3389/feart.2016.00086>
- Yuill, R. S. (1971). The standard deviational ellipse: An updated tool for spatial description. *Geografiska Annaler*, 53(1), 28–39. <https://doi.org/10.1080/04353684.1971.11879353>

References From the Supporting Information

- Cancel Vazquez, S. M., Rooney, T. O., Brown, E. L., Bollinger, A., Bastow, I. D., Steiner, R. A., & Kappelman, J. (2024). Basaltic pulses and lithospheric thinning—Plio-pleistocene magmatism and rifting in the Turkana depression (East African rift system). *Journal of Geophysical Research: Solid Earth*, 129(8), e2024JB029166. <https://doi.org/10.1029/2024JB029166>
- Heidbach, O., Rajabi, M., Cui, X., Fuchs, K., Müller, B., Reinecker, J., et al. (2018). The world stress map database release 2016: Crustal stress pattern across scales. *Tectonophysics*, 744, 484–498. <https://doi.org/10.1016/j.tecto.2018.07.007>